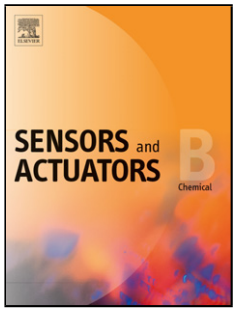

Title: Combined in vivo recording of neural signals and iontophoretic injection of pathway tracers using a hollow silicon microelectrode

Author: Z. Fekete E. Pálfi G. Márton M. Handbauer Zs. Bérces I. Ulbert A. Pongrácz L. Négyessy

PII: S0925-4005(15)30823-6
DOI: http://dx.doi.org/doi:10.1016/j.snb.2015.12.099
Reference: SNB 19500

To appear in: *Sensors and Actuators B*

Received date: 2-10-2015
Revised date: 18-12-2015
Accepted date: 29-12-2015

Please cite this article as: Z.Fekete, E.Pálfi, G.Márton, M.Handbauer, Zs.Bérces, I.Ulbert, A.Pongrácz, L.Négyessy, Combined in vivo recording of neural signals and iontophoretic injection of pathway tracers using a hollow silicon microelectrode, Sensors and Actuators B: Chemical http://dx.doi.org/10.1016/j.snb.2015.12.099

Combined in vivo recording of neural signals and iontophoretic injection of pathway tracers using a hollow silicon microelectrode

Z. Fekete[1*#], E. Pálfi[2,3*], G. Márton[4], M. Handbauer[1,5], Zs. Bérces[1,5], I. Ulbert[4,5], A. Pongrácz[1,6], L. Négyessy[2,3]

[1]MTA EK NAP B Research Group for Implantable Microsystems, 29-33 Konkoly-Thege st, Budapest, H-1121, Hungary

[2]Complex Systems and Computational Neuroscience Group, Wigner Res. Cen. for Physics, 29-33 Konkoly-Thege st, Budapest, H-1121, Hungary

[3]Department of Anatomy, Histology and Embryology, Semmelweis University, 58 Tűzoltó st, Budapest, H-1094, Hungary

[4]Institute of Cognitive Neuroscience and Psychology, Research Centre for Natural Sciences, Magyar tudósok krt 2, Budapest, H-1117, Hungary

[5]Department of Information Technology and Bionics, Pázmány Péter Catholic University, 50/A Práter str, Budapest, H-1083, Hungary

[6]Neuromicrosystems Ltd, 29-33 Konkoly-Thege st, Budapest, H-1121, Hungary

*Authors equally contributed.

[#]Corresponding author.

Highlights

1. Spatially controlled neuronal labeling is performed with a hollow silicon microelectrode

2. Combination of iontophoretic injection with electrophysiology using a single micromachined device is demonstrated in acute animal experiment

3. Mapping the projectome of locally labeled neuronal population is demonstrated as possible application of microiontophoresis function of a silicon neural probe.

Abstract

This paper presents the results of in vivo local release of a neuronal tracer, biotinylated dextran amine (BDA) in the rat somatosensory cortex using monolithically integrated microfluidic channel of a silicon neural microelectrode. The tracer injection is controlled by iontophoresis using Pt electrodes in the vicinity of the outlet of the microfluidic channel. Using 3-5 μA, 5-7 s on/off cycle and 15-20 min total injection time the localized injection resulted in clear anterograde and retrograde BDA labeling both within the cortex and in subcortical structures. Anterograde and retrograde labeling revealed the fine details of neuronal processes including dendritic spines and axon terminal-like endings. Injection sites appeared clear lacking any strong diffuse background labeling. Electrophysiological recording performed with the same microdevice immediately after the iontophoresis indicated normal cortical functioning. The results prove that the combination of in vivo multichannel neural recording and controlled tracer injection using a single implanted microdevice is feasible, and therefore it can be a powerful tool for studying the connectome of the brain.

1. Introduction

Thorough investigation of the brain's wiring diagram is essential for understanding neural information processing at both local and global scales [1]. Exploring the structure and function of the brain's connectome is in fact one of the major scope of recent neuroscience research. However, new methods and technologies need to be developed to bridge brain structure and function [2]. Complementing neuronal recording with pathway tracing is still an indispensable tool to achieve such goals specifically at the microcircuit (single neurons) and mesoscale (neuronal populations) levels of the neural network. However, electrophysiology and neuronal tract tracing are usually applied separately even if combined in the same experiment. Typically if recording of neural activity is also needed, an additional electrode is positioned into the investigated brain area close to the micropipette or glass capillary used for neuronal labelling [3]. Similarly, the sequential application of electrode recording and tracer injection within the same experiment has several shortcomings including precision issues (targeting the same tissue volume), increased tissue damage by multiple penetrations, long preparation of electrode configurations. There are several drawbacks of such an approach including the precise alignment of the different electrodes/syringes, crowded instrumentation and the invasive manner of the surgery. Therefore a device integrating both microelectric recording and tract tracing capabilities is highly demanded to enhance efficiency and precision of such a multidisciplinary approach. Also, using integrated devices simplifies the experimental procedures and would perhaps increase the popularity of experiments combining physiological and anatomical approaches. Such progress could ultimately provide significant contribution in understanding the connectome [4].

In vivo intra- and juxtacellular recordings are usually made by electrodes filled with substances as e.g. biocytin, allowing the subsequent anatomical reconstruction of the neurons. These are important tools in exploring the neuronal microcircuitry. However, recent development in the field of multielectrode recording (MUR) provides new opportunities in examining mesoscale, population level functional and structural (spatial patterns) phenomena. Also, understanding the neural basis of MUR related phenomena requires knowledge about the underlying neuronal connectivity. Anterograde and retrograde tracing techniques are fundamental means of connectional neuroanatomy [5]. There are numerous substances used for tracing with varying chemical properties (6]. Biotinylated dextran amine (BDA) is one of the most popular tracers because of its sensitivity and the ease of use for different purposes including fluorescence and electron microscopy. BDA is widely used for labeling the origin as well as the termination of neural connections [4]. High molecular weight BDA (<10 kDa) yields higher anterograde sensitivity and provides detailed labeling of axons and terminals (target regions), while low molecular weight BDA (>3 kDa) yields higher sensitivity and provides detailed retrograde labeling of neuronal cell bodies (origin of pathways) [4]. However, it should be noted that in some amount BDAs of different molecular weights are transported in both directions and that the preference of direction can be controlled for some extent with the experimental procedures applied (method of injection, combined neurochemical lesion with

NMDA, survival time etc.)[7].

BDA has been used to trace connections both within the cerebral cortex and between cortical and subcortical structures of different species. BDA labelling revealed projections from numerous regions in the CNS, e.g. from the cortex to the substantia nigra [8], from the brainstem [9], medulla [10], thalamus [7] etc. The two point source diffusion based real time techniques for drug delivery are iontophoresis and pressure ejection, both from a micropipette [11]. BDA can be applied both by pressure and iontophoresis. Iontophoresis is a fundamental technique to eject charged molecules including neuronal tracers in the brain tissue through establishing voltage gradient between the tracer solution suspended in a micropipette and the extracellular space. The advantage of iontophoresis over pressure injection is that ions and not the solution can be released in a modest amount by controlling the iontophoretic current [11]. The polarity of the applied current depends on the charge of the substance to be injected by iontophoresis. If there are no further charged molecules in the solution, then the amount of tracer deposited in the tissue is proportional to the total charge delivered by the current source. This implies that the electric current and injection time are the relevant parameters to be precisely controlled in an experiment. Mostly, pulsed direct current is used to prevent impedance build-up in micropipettes. One of the electrodes is a fine gauge wire which is inserted in the micropipette shaft. For this purpose, gold wire, silver wire, chloridized silver wire or stainless steel wire have been used. The other (reference) electrode is usually connected to some arbitrary site of the animal body, mostly outside of the brain tissue, providing a practically homogenous voltage gradient throughout the corpus of the animal.

In recent years, neural microelectrodes of several functionality have been developed and demonstrated [12-14]. For convection enhanced drug delivery purposes, a variety of microdevices has been successfully tested in vivo [15-19]. In our work, we propose an in vivo method of using neural microelectrode with monolithically integrated microfluidic channel to control tracer delivery in the close vicinity of the recording sites by iontophoresis. Additionally, we also prove that recording functionality is still facilitates the monitoring of local field potentials, single- and multiple unit activity. Detailed description of the device fabrication and application for convection enhanced delivery of drugs through the blood brain barrier can be found in our previous work [15].

2. Experimental methods

2.1 Design & fabrication of the microfluidic channel and the microelectrodes

The fabrication of the microelectrode is based on standard silicon MEMS process described in this section. The fabrication process can be found in details in [15, 20]. First, the buried microchannel is fabricated then the functional layers and the probe shaft were micromachined. The initial substrate is a 380 μm thick (100) single-crystalline silicon wafer. Thermally grown dry silicon-dioxide and standard Microchem 1818 photoresist were used as a masking material for Si etching. Silicon dioxide was patterned in $C_4F_8 + O_2$ plasma using reactive ion etching. Deep trench etching (Bosch process) in silicon was carried out in an Oxford Plasmalab System 100

chamber at room temperature. After removing the photoresist, an additional 100 nm thick SiO_2 was thermally grown on the substrate and on the trench walls. Electron beam evaporation of a 100 nm thick Al layer follows the oxidation, which acted as a protective coating during selective SiO_2 removal from the bottom of the trench. In order to remove the SiO_2 protective layer from the bottom of the trench, an anisotropic etch recipe using CHF_3 + Ar plasma chemistry is utilized. The formation of microchannels (isotropic Si etch) was carried out in SF6 plasma. In order to remove the sidewall protection, buffered HF was used for wet chemical etching of both Al and SiO_2 protection layers. After dehydration of the wafers at 300°C, an LPCVD process is applied for filling the microchannels and completely sealing the trenches by 1500 nm poly-Si deposition at 630°C. The formation of the buried microchannel is explained in more detail in [21]. Silicon wafers containing the buried microchannels were oxidized in wet atmosphere at 1100 °C in order to grow a 50nm thick thermal SiO_2 layer on the substrate surface. To further isolate the recording sites from the bulk Si, a 300nm thick low-stress silicon nitride (SiN_x) film was then deposited on top of the SiO_2 by LPCVD at 830 °C. A sacrificial Al layer was used to define the pattern of the TiO_x/Pt recording sites and conductor paths via a standard lift-off process. First, the 300nm thick sacrificial Al layer was deposited by electron beam evaporation. This was followed by the first photolithography and etching steps defining the inverse pattern of the conductor path. The conductor layer consisted of a 15 nm thick adhesion layer of TiO_x formed by reactive sputtering of Ti in an Ar/O_2 atmosphere. In the same vacuum cycle, 270 nm thick Pt was sputtered on top of TiO_x. The photoresist together with the overlying TiO_x/Pt layer was removed using acetone. The Al layer was etched away as before, to complete with the lift-off process. In the next step the upper passivation stack is formed, 300 nm thick SiO_2 and SiN_x layers were deposited using LPCVD at 430 °C and 830°C, respectively. Contact and bonding sites were defined by additional photolithography step followed by selective SiO_2 and SiN_x wet etching process in NH_4F buffered HF and phosphorous acid until the total removal of the oxide and nitride layers. The probe shaft and inlet reservoirs were micromachined by dry etching using Bosch recipe in an Oxford Plasmasab System 100 DRIE chamber. Masking layer was standard photoresist on the front side, while the etch stop layers were electron beam evaporated Al film and subsequently spin-coated photoresist. The fabrication process can be found in more details in [15, 20].

The monolithically integrated microfluidic channel is 15 mm long, and 314 μm^2 in cross-section. The fluidic outlets are on the side of the probe as presented on Fig. 1.a. The counter Pt electrode is 900 μm^2 and the distance between the fluidic outlet and the Pt counter electrode is 125 µm. Schematic layout of the probe tip is shown in Fig 1.b. The fluidic interfacing to the probe is described in our previous work in details [15].

2.2 Surgery

Animal care and experiments were performed in compliance with Animal Care Regulations of the Institute for Psychology of the Hungarian Academy of Sciences and order 243/1988 of the

Hungarian Government, which is an adaptation of directive 86/609/EGK of the European Committee Council. The animals were initially anesthetized via intraperitoneal injection of a mixture of 37.5 mg/ml ketamine and 5 mg/ml xylazine at 0.3 ml/100 g body weight injection volume. The sleeping state was maintained by intramuscular updates of the same solution. A drop of paraffin oil was applied in each eye of a rat in order to prevent them from drying. The anesthetized animal was placed into a stereotactic frame (David Kopf Instruments, Tujunga, CA, USA), head-restrained. The scalp and other soft tissues, including the periosteum covering the skull were removed with a scalpel. Craniotomy window was opened above the parietal lobe. The dura mater was incised and removed with a sharp needle. Also, the arachnoid membrane and the pia mater were gently poked with a fine needle tip.

2.3 In vivo extracellular recording

Electrophysiological recording was performed following the iontophoretic injections. At the same location, the probe was utilized for multichannel extracellular recording, using a two-stage amplifier and a data acquisition system with a gain of 1000, 20 kHz sampling rate and 16 bit resolution (LabView, National Instruments Corp., Austin, TX, USA) [22]. Edit 4.5 software of Neuroscan (Charlotte, NC, USA) was used for off-line signal visualization, filtering and analysis. The Klusters free software was used for clustering unit activities [23].

2.4 Iontophoretic injection of BDA

In six cases (REF, LF1, MF1, MF2, HF1, HF2) a 1:1 mixture of high and low molecular weight 10% BDA (MW 10.000 and 3000, final cc 5 % each) (Molecular Probes, Inc. Eugene, OR, USA) dissolved in 0.01M phosphate buffer (pH 7.4) were used. These studies were evaluated through histology examinations only (see Table 1). In three further cases (REF2, PR, PRELFIZ)we used only the BDA 10K in 10% to test neuronal labeling followed by electrical recording through the same device (see Table 2.).The fluidic channel was filled with the BDA solution prior to the surgery. The counter Pt electrode, one among the recording sites of the multielectrode array (MEA) near to the opening of the channel on the shaft, was negatively biased relative to the channel containing the BDA, while the electrical current was measured. A positively biased silver electrode was placed into the fluidic channel to repel the positively charged BDA molecules out of the drug delivery channel. A control experiment was carried out without any voltage bias (injector turned off) allowing passive diffusion between the microfluidic channel and the extracellular space. Each injection lasted for 15 minutes and was applied by varying the length of the on/off cycle and the current amplitude. Injections were made at different depths (660-1440 μm) depending on electrode configurations (Table 3).

2.5 Perfusion

After 7 days survival period, animals were deeply anesthetized before perfusing transcardially with 300 ml of 0.9 % NaCl in distilled water and 500 ml fixative consisted of 4%

paraformaldehyde in 0.1M PB (pH 7.3). Brains were immediately removed and the region of interest was then cut from the cortex, flattened and postfixed for an hour in cases REF, LF1, MF1, MF2, HF1, HF2. Cases REF2, PR and PRELFIZ were just postfixed for an hour.

2.6 Histology and microscopy

Following dissection of the region of interest, serial sections were cut at 60 µm either in the horizontal (cases REF, MF1, MF2, HF1, HF2, LF1) or in the coronal plane (cases REF2, PR, PRELFIZ) with a vibratome. The standard ABC protocol (Elite kit, Vector Laboratories, Inc. Burlingame, CA, USA) was used to visualize BDA labeling with Nickel enhanced diaminobenzidin (Ni-DAB) (Sigma-Aldrich Kft, Budapest, Hungary) as the chromogen. In short, sections were rinsed in 0.1 M PB and first treated with 0.5% Triton-X 100 (Reanal Zrt., Budapest, Hungary) in 0.1 M PB for 30 minutes. After a several washes in 0.1 M PB, intrinsic peroxidase activity was blocked by 1% H_2O_2 in PB (30 min) before the ABC step. The sections were incubated with the avidin/biotinylated enzyme complex (ABC, 1:200 in PB, 0.1M, pH 7.4) for 2 hours at room temperature and washed thoroughly. After the Ni-DAB reaction the sections were mounted on gelatinated slides and cover slipped with Depex (Serva Electrophoresis GmbH, Heidelberg, Germany).Images were collected with an Olympus research microscope equipped with a motorized stage (MultiControl 2000, Märzhäuser Wetzlar GmbH & Co. KG, Wetzlar, Germany) using the 2D Virtual Tissue module of Neurolucida® (Micro Bright Field Europe, E.K. Magdeburg, Germany). Except some enhancement of the contrast and brightness microscopic images were not edited.

3. Results & Discussion

Several successful iontophoretic injection were carried out using the microfluidic channel of the neural microelectrode. The implantation of the microelectrodes resulted in some tissue damage at the injection site, which however, apparently did not affect the injection and transport of BDA. In general, the applied mixture of high and low molecular weight BDA provided a clear labeling of neuronal cell bodies and terminals that are present in the vicinity of the implantation track. A representative microscopic view of a labeled neuron is shown in Figure 2.c. BDA labeled neurons were clearly recognizable at the site of injection, which was devoid of a strong diffuse background labeling.

3.1 Control experiment

To avoid any artifacts in our measurements, we carried out control in vivo experiments to reveal the extent of diffusion of the tracer molecules through the outlet of the fluidic channel. Comparison of the control experiment and the iontophoretic injection is shown in Figure 2 and Figure 3. In the control case, where no current was used we did not find any labeled structures. In case of iontophoresis, we found anterogradely labeled axons and retrogradely labeled neurons. Although, in bidirectional tracing we have to consider the possibility of axonal

backfilling in retrogradely labeled neurons, which could be mistakenly identified as anterograde labeling from the injection site. However, we found dense axonal labeling distant from retrogradely labeled neurons, which suggest that our bidirectional tracing worked effectively. More detailed discussion of this methodological issue can be found in [7].

3.2 Effect of the injection parameters on BDA labeling

Detectable BDA labeling was observed only when applying current amplitude, length of the on/off cycle and total injection time described by previous studies using glass capillary electrodes [7]. Accordingly, 3-5 μA, 5-7 s on/off cycle and 15-20 min total injection time resulted in nice anterograde and retrograde BDA labeling both within the cortex as well as in subcortical structures. Interestingly, injection sites appeared very clear lacking the strong diffuse labeling characterizing the core region of iontophoretic injections and only a thin halo area was observed (Figure 2, see Table 3). No noticeable difference was observed in the BDA labeling when using the different types of electrode configurations.

3.3 Mapping the projectome of the primary somatosensory cortical trunk region by BDA

Figure 4 shows examples of anterograde and retrograde BDA labeling in distant cortical and subcortical areas including the ipsilateral cortico-cortical, callosal and thalamic connections. In another case in Figure 5, we show the laminar columnar organization of long distance lateral cortical connections. In all cases both anterograde and retrograde labeling revealed the fine details of neuronal processes including dendritic spines and axon terminal-like endings (Figs. 1C-F, 2C,D).

3.4 Recording of neural activity

The probes were suitable for the detection of neurophysiological signals. Figure 6 shows samples of recordings, obtained after iontophoretic tracer release. The probe was slowly extracted from the tissue with 800 μm steps. After the second step, its proximal site reached the brain surface. High quality local field potential, single and multiple unit activities could be measured. Figure 7 A and B shows examples for single units (spikes), detected at the place of the tracer release and 800 μm above it, respectively.

3.5 Perspective of applications

In vivo iontophoresis in the central nervous system is mostly applied to deliver dyes and pathway tracers for subsequent histological studies [4, 7, 23] or to investigate the effect of drugs on neuronal activity [24-26]. These studies relies on the application of pulled glass micropipettes [24-25] or multi-barreled carbon fiber electrodes [27-28]. The combined use of iontophoresis and single cell electrophysiology is apparently necessary in these neuropharmacological studies, however, potential measurements are only based on one

recording site only. Our proposed device facilitates the parallel use of local iontophoresis and multi-electrode recording offering the observation of multiple neurons or neuronal populations along the probe track with limited tissue damage. Besides pathway tracing, we envision to exploit such advantage in fundamental behavioural animal studies in the future as well.

4. Conclusion

In this paper, the successful application of a monolithically integrated microfluidic channel in a neural microelectrode for local iontophoretic drug delivery and neuronal labeling is demonstrated in vivo. The localized injection using 3-5 μA, 5-7 s on/off cycle and 15-20 min total injection time resulted in clear anterograde and retrograde BDA labeling both within the cortex as well as in subcortical structures providing the projectome of the primary somatosensory cortical trunk area. In all cases, both anterograde and retrograde labeling revealed the fine details of neuronal processes including dendritic spines and axon terminal-like endings. Injection sites appeared very clear lacking the strong diffuse labeling characterizing the core region of iontophoretic injections and only a thin halo area was observed. No BDA labeling was found in control experiments, where the iontophoresis device was not turned on. Combined tracer injection and electrophysiology is presented in anaesthized animals using the very same microprobe. Tracer injection did not result in abnormal cortical functioning examined by electrophysiological recordings. Since the proposed device is feasible to serve combined labeling and electrophysiology studies with precisely (micron resolution) defined fluidic outlet and recording site relative positioning, we envision further applications like neural microcircuit and projectome mapping in animal studies.

Acknowledgement

The authors are thankful to the Hungarian Brain Research Program (KTIA NAP 13-2-2015-0004 and KTIA 13 NAP A IV/6) and the National Research, Development & Innovation Office (TÉT_14_FR-1-2015-0030). Anita Pongrácz and Zoltán Fekete are grateful for the support of Bolyai János Scholarship and the Return Fellowship granted by the HAS and the Alexander von Humboldt Foundation, respectively.

Author Biography

Zoltán Fekete received Master and Ph.D. degrees in Electrical Engineering in 2009 and 2013, respectively, from the Budapest University of Technology and Economics, in Hungary. His research interests lie in the development of silicon MEMS devices for biomedical applications including novel neural interfaces. In 2013, he was awarded an Alexander von Humboldt Fellowship for postdoctoral researchers. As a post doc in the Department of Microsystems Engineering (IMTEK) at the University of Freiburg, he focused on the micro- and nanofabrication of novel 3D microelectrode arrays for high

density optogenetic stimulation. From 2015, he is acting as principal investigator of the Research Group for Implantable Microsystems (neuroMEMS), Centre for Energy Research, Hungarian Academy of Sciences.

Emese Pálfi received her Msc in neurobiology from the Eötvös Lóránd University in 2012. She is currently working toward her PhD degree in neuroscience at the Semmelweis University, Budapest. She devotes her research to reveal the role of the cortical inhibition in primate somatosensory cortex.

Gergely Márton received the MSc degree in electrical engineering from the Budapest University of Technology and Economics (BUTE) in 2010. He is currently working toward the PhD degree in neuroscience at the Semmelweis University Doctoral School. His main interest is the experimental investigation biomedical microdevices in the central nerbous system.

Máté Handbauer received his Msc degree in bionic engineering from the Pázmány Péter Catholic University (PPCU) in Budapest in 2015. He focused on the microfluidic characterization of implantable microdevices.

Zsófia Bérces received her MSc degree in bionic engineering from the Pázmány Péter Catholic University (PPCU) in Budapest in 2013. Her main interests include the electrochemical characterisation of MEMS devices and the effects of surface nanostructuring in neurobiological applications. She is working towards a PhD at the Institute of Technical Physics & Material Science, CER, HAS.

István Ulbert is associate professor at Peter Pazmany Catholic University and Institute of Cognitive Neuroscience and Psychology, CNRS, HAS. He received his MSc degree in electrical engineering from the Technical University of Budapest in 1988, the MD degree from the Semmelweis University Medical School in 1997 and the PhD degree in neuroscience from the Semmelweis University Doctoral School in 2002. His main interests are the following: development of implantable cortical biosensors, amplifier and interconnecting systems and analysis tools, investigation of intracortical generators of evoked potentials and epilepsy and investigation of the relationship of electrical and hemodynamic responses in cortical structures.

Anita Pongrácz received her MSc degree in engineering physics in 2004 from the Technical University of Budapest, Hungary. In 2006–2007 she worked as a baseline process engineer in the UC Berkeley Microfabrication Laboratory. Her main responsibilities were to design, fabricate, test, and evaluate CMOS test devices. She received her PhD in 2010 and currently she is a research fellow at the Institute of Technical Physics and Material Science, Centre for Energy Research, Hungarian Academy of Sciences. Her research interests include microfabrication of NeuroMEMS devices.

László Négyessy is an associate professor at Semmelweis University and at the Complex Systems and Computational Neuroscience Group, Wigner Centre for Physics, HAS. He received his MD in biology from the Eötvös Lóránd University, Budapest in 1993, and his PhD in neuroscience from the University of Pécs, Hungary. His research interest include organization and plasticity of cortical networks, modeling

large scale cortical integration and the role of the tissue non-specific alkaline phosphatase in neuronal transmission.

References

[1] A. W. Toga, K. A. Clark, P, M. Thompson, D. W. Shattuck, J. D. Van Horn, Mapping the human connectome, Neurosurgery 71 (2012) 1-5

[2] P. Osten, T. W. Margrie, TW, Mapping brain circuitry with a light microscope, Nat. Meth. 10, (2013) 515-523

[3] S. Davidson, H. Truong, Y. Nakagawa, G. J. Giesler, A microinjection technique for targeting regions of embryionic and neonatal mouse brain in vivo, Brain Res. 1307 (2010) 43-52

[4] S. W. Oh, et al, A mesoscale connectome of the mouse brain, Nature 508 (2014) 207–214

[5] E. Oztas, Neuronal tracing, Neuroanatomy 2 (2003) 2-5.

[6] J. L. Lanciego, F. G. Wouterlood, A half century of experimental neuroanatomical tracing, J Chem. Neuroanat. 42 (2011) 157-183

[7] L. Négyessy, P. S. Goldman-Rakic, Morphometric characterization of synapses in the primate prefrontal cortex formed by afferents from the mediodorsal thalamic nucleus, Exp Brain Res. 164 (2005) 148-154

[8] A. Naito, H. Kita, The cortico-pallidal projection in the rat: an anterograde tracing study with biotinylated dextran amine, Brain Res. 637 (1994) 317-322

[9] A. L. Halberstadt, C. D. Balaban, Anterograde tracing of projections from the dorsal raphe nucleus to the vestibular nuclei, J Neurosci 143 (2006) 641–654

[10] H. Leite-Almeida, A. Valle-Fernandes, A. Almeida, Brain projections from the medullary dorsal reticular nucleus: an anterograde and retrograde tracing study in the rat, J Neurosci 140 (2006) 577–595

[11] A. C. Michael, L. Borland, Electrochemical Methods for Neuroscience, CRC Press, 2006

[12] K. D. Wise, A. M. Sodagar, Y. Yao, M. N. Gulari, G. E. Perlin, K. Najafi, Microelectrodes, Microelectronics, and Implantable Neural Microsystems, Proc. IEEE, Special Issue on Implantable Biomimetic Microelectronic Systems 7 (2008) 1184-1202

[13] Z. Fekete, Recent advances in silicon-based neural microelectrodes and microsystems: a review, Sens & Act. B: Chemical 215 (2015a) 300-315

[14] G. Buzsáki, E. Stark, A. Berényi, D. Khodagholy, D. R. Kipke, E. Yoon, K. D. Wise, Tools for

probing local circuits: High-density silicon probes combined with optogenetics, Neuron 86 (2015) 92-105

[15] A. Pongrácz, Z. Fekete, G. Márton, Z. Bérces, I. Ulbert, P. Fürjes, Deep-brain silicon multielectrodes for simultaneous in vivo neural recording and drug delivery, Sens & Act B: Chemical 189 (2013) 97–105

[16] H. J. Lee, Y. Son, D. Kim, Y. K. Kim, N. Choi, E. Yoon, I. Cho, A new thin silicon microneedle with an embedded microchannel for deep brain drug infusion" Sens. & Act. B: Chemical 209 (2015) 413-422

[17] A. Altuna, J. Berganzo, L. J. Fernández, Polymer SU-8-based microprobes for neural recording and drug delivery, Front. in Mat. 2 (2015) 47.

[18] H. Shin, H. J. Lee, U. Chae, H. Kim, J. Kim, N Choi, I. J. Cho, Neural probes with multi-drug delivery capability, Lab on a Chip, 15 (2015) 3730-3737

[19] S. Spieth O. Brett, K. Seidl, A. A. Aarts, M. Erismis, S. Herwik, F. Trenkle, S. Tatzner, J. Auber, M. Daub, H. P. Neves, R. Puers, O. Paul, P. Ruther, R. Zengerle, A floating 3D silicon microprobe array for neural drug delivery compatible with electrical recording, J. Micromech. Microeng. 21 (2011) 125001.

[20] Z. Fekete, Technology of ultralong deep brain fluidic microelectrodes combined with etching-before-grinding, Microsyst. Technol. 21 (2015b) 341-344

[21] Z. Fekete, A. Pongracz, P. Fürjes G. Battistig, Improved process flow for buried channel fabrication in silicon, Microsyst.Tech. 18 (2012) 353-358

[22] I. Ulbert, E. Halgren, G. Heit, G. Karmos, Multiple microelectrode-recording system for human intracortical applications, J Neurosci Meth. 106 (2001) 69-79

[23] L. Négyessy, V. Gál, T. Farkas, J. Toldi, Cross-modal plasticity of the cortico thalamic circuits in rats enucleated on the first postnatal day, Eur J Neurosci. 12 (2000) 1654-1668

[24] L. Hazan, M. Zugaro, G. Buzsaki, G, Klusters, NeuroScope, NDManager: a free software suite for neurophysiological data processing and visualization, J Neurosci. Meth. 155 (2006) 207-216

[25] A. Bacq, L. Balasse, G. Biala, B. Guiard, A. M. Gardier, A. Schinkel, F. Louis, V. Vialou, M. P. Martres, C. Chevarin, M. Hamon, B. Giros, S. Gautron, Organic cation transporter 2 controls brain norepinephrine and serotonin clearance and antidepressant response, Molecular

Psychiatry 17 (2012) 926-939

[26] F. R. Bambico, B. Lacoste, P. R. Hattan, G. Gobbi, Father Absence in the Monogamous California Mouse Impairs Social Behavior and Modifies Dopamine and Glutamate Synapses in the Medial Prefrontal Cortex, Cereb. Cortex first published online December 4, 2013 doi:10.1093/cercor/bht310

[27] M. Mansari, M. Lecours, P. Blier, Effects of acute and sustained administration of vortioxetineon the serotonin system in the hippocampus: electrophysiological studies in the rat brain, Psychopharmacology 232 (2015) 2343–2352

[28] Z. K. Bali, D. Budai, I. Hernádi, Separation of electrophysiologically distinct neuronal populations in the rat hippocampus for neuropharmacological testing under in vivo conditions, Acta Biol Hung. 65 (2014) 241-251

[28] A. M. Belle, C. Owesson-White, N. R. Herr, R. M. Carelli, R. M. Wightman, Controlled iontophoresis coupled with fast-scan cyclic voltammetry/electrophysiology in awake, freely moving animals, ACS Chem. Neurosci 4 (2013) 761-771

Figure Captions

Figure 1.a. SEM image of a multichannel silicon neural electrode with 12 Pt contact sites on the top surface and two buried microfluidic channels. The outlets of the channels are on the sidewalls. b: Schematic layout of the probe. Light blue lines represents the centre of the buried microfluidic channels. Dark blue regions are the Pt recording sites and wiring. The first Pt electrode was used as counter electrode during iontophoretic injection of BDA. The Pt sites are 30x30µm^2.

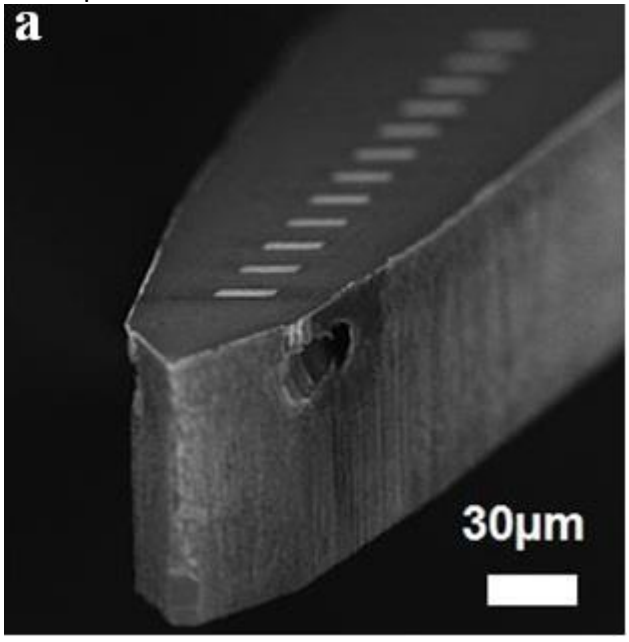

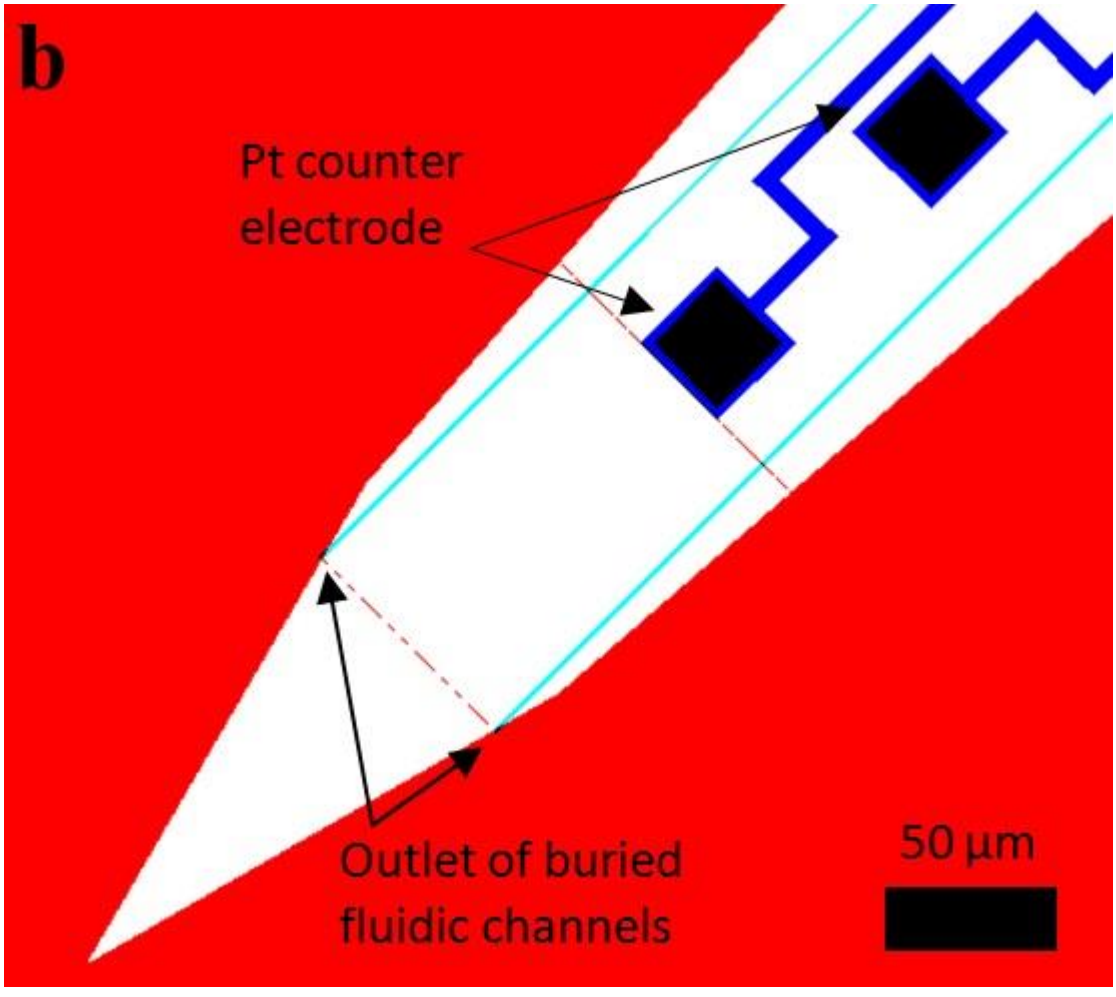

Figure 2. BDA labeling of neurons after iontophoretic injection is shown on tangential sections. Greyscale images taken with a light microscope. Stars indicate the electrode track. a, In case of MF1, BDA injection resulted in the retrograde labeling of neuronal perikarya (black arrows) in the vicinity of the injection site. Arrow head groups show the halo region around the injection site. b. No BDA labeled neurons were found in the control (case REF is shown). Note tissue damage at the electrode track. Scale bar: 250 µm. c. Close microscopic view of a labeled pyramid cell. Scale bar is 15 µm.

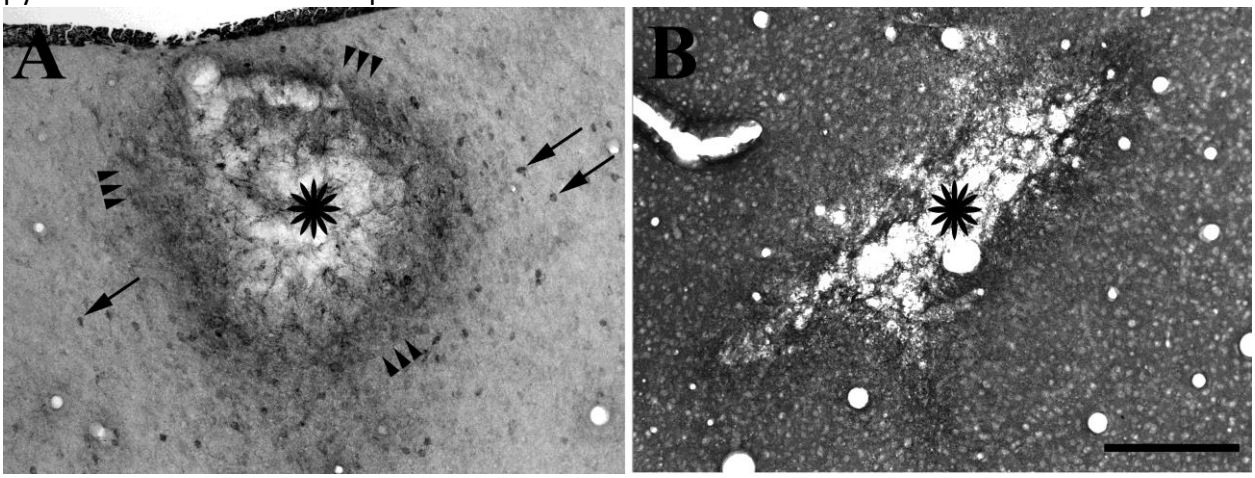

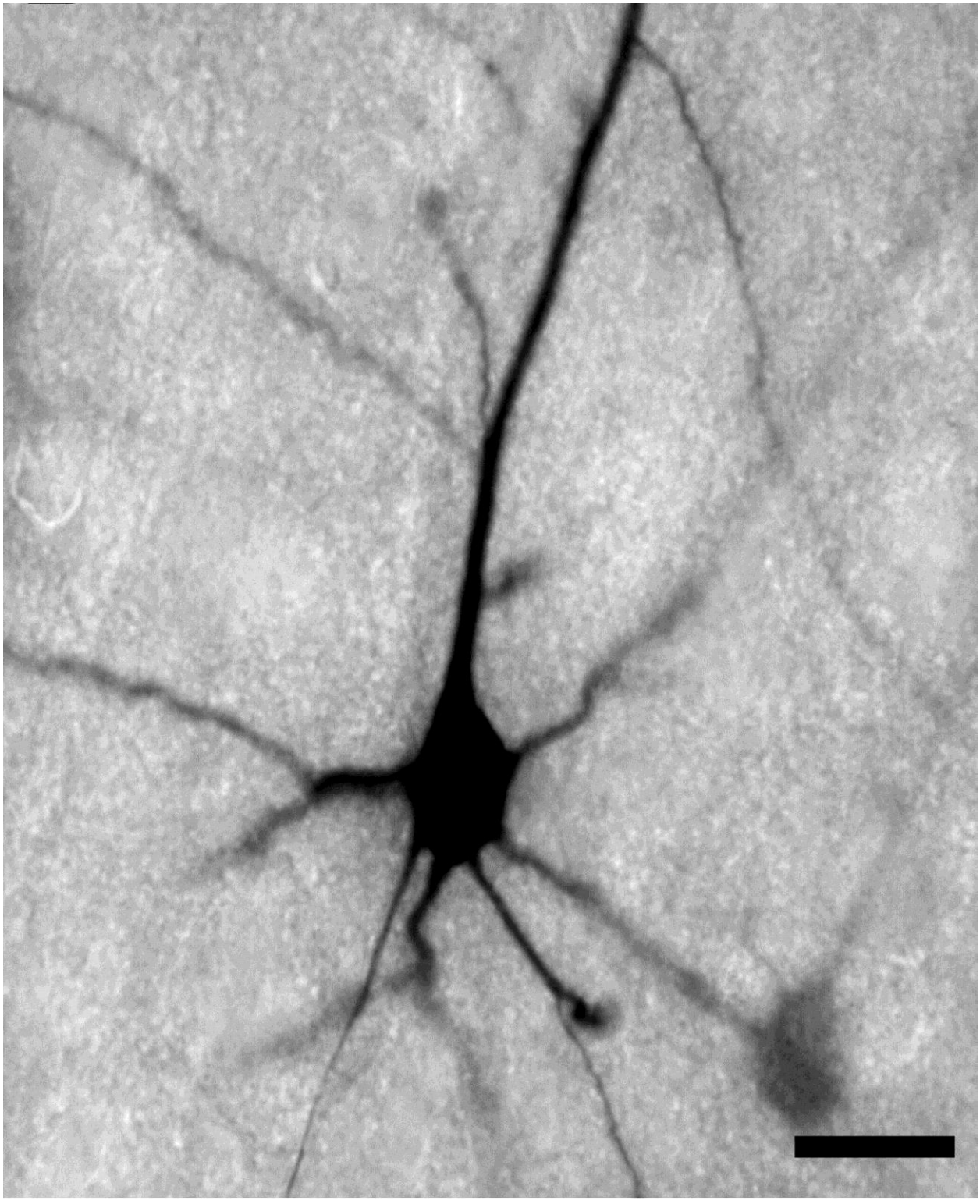

Figure 3. Lack of BDA labeling in the control experiment (case REF2). A) Coronal section through the electrode track. Black arrow shows the injection site. orientation: D-dorsal, L-lateral. Scale bar represents 1 mm. B) Neither anterograde nor retrograde BDA labeling appeared at the injection site. Scale bar represents 100 µm.

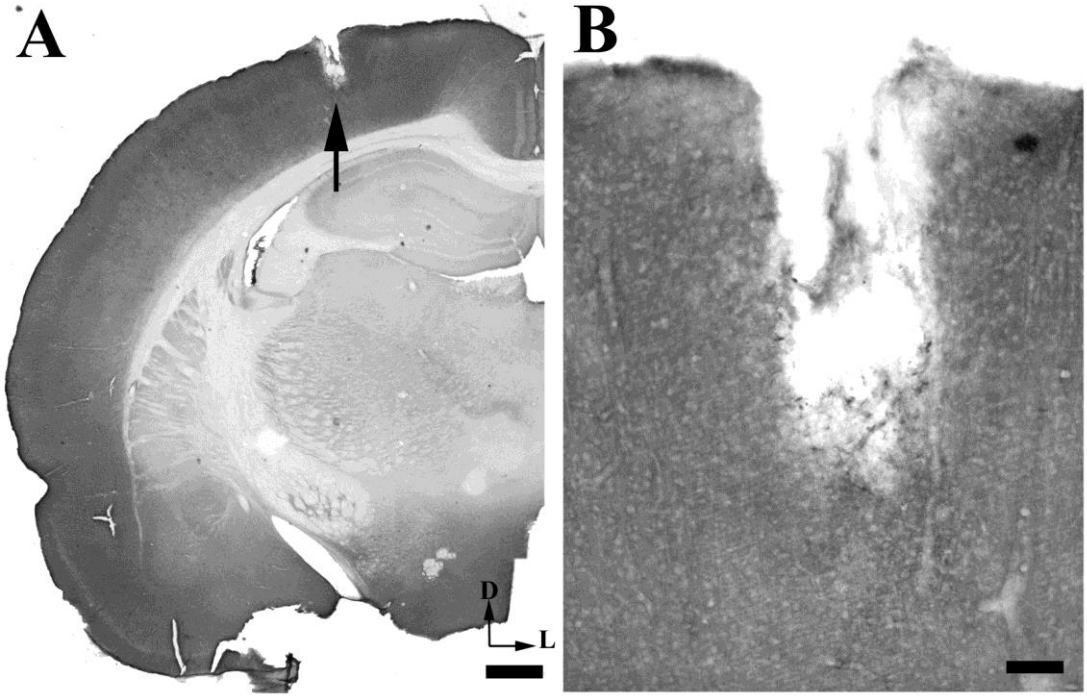

Figure 4. Retrograde and anterograde BDA labeling in the cerebral cortex and the thalamus. A) Coronal section of the brain through the injection site (B) in case PRELFIZ. *B-F)* indicate the sites where images enlarged on the corresponding panels B-F, were taken from. Orientation: D-dorsal, L-lateral. Scale bar represents 1 mm. B) Injection site. Black points represent the cell bodies of the BDA labeled neurons. Note the bilaminar accumulation with one group of labeled somata near the cortical surface (top of the image) and another in the middle layers shown in the center of the image. Note also the apical denrites represented by the numerous parallel, thin processes originating from the BDA labeled neurons of the middle layers and running upward. Scale bar represents 100 µm. C) Labeled neurons (black arrows) and axons (white arrows) in the cortex. Contrast inverted to enhance visibility. Scale bar represents 100 µm. D) BDA labeled callosal neurons (black arrows) on the cortical hemisphere contralateral to the injection site. Scale bar represents 100 µm. E) BDA labeled axons (white arrows) in the thalamus. Inverted image. Scale bar represents 50 µm. F) Retrogradely labeled neurons (black arrow) in the thalamus. Scale bar represents 50 µm.

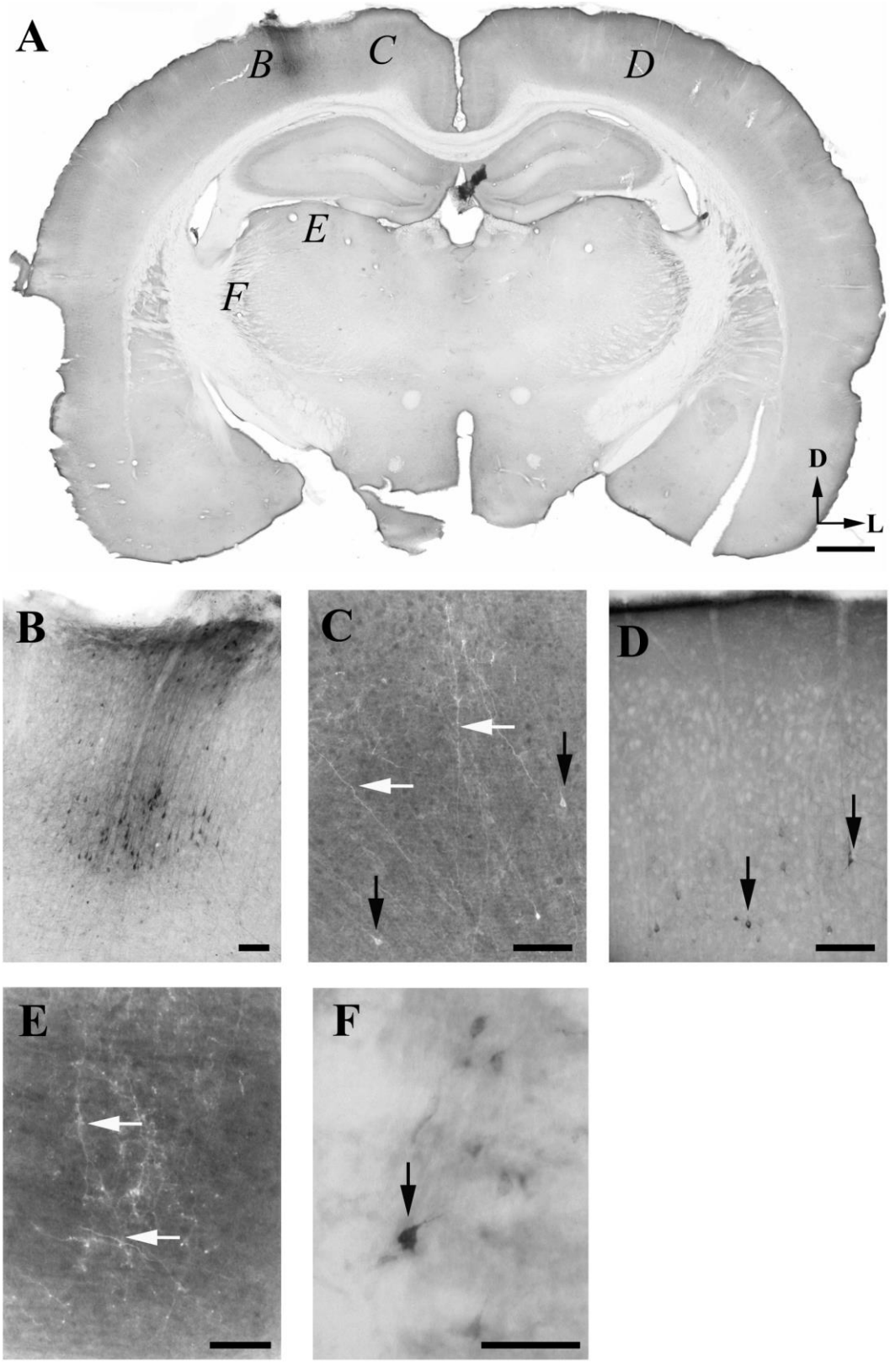

Figure 5. Columnar appearance of the BDA labeled cortico-cortical connections in case PR. A) Coronal section through the injection site (black arrow). Note BDA labeling almost along the full depth of the cortex. Orientation: D-dorsal, L-lateral. Scale bar: 1 mm. B) BDA labeled neuronal cell bodies (black dots) are present all along the electrode track and accumulate in the deep layers. Note the lack of a dense tracer deposit and that the labeled neurons are clearly distinguishable. Inset: enlarged image of the area in the rectangle showing a BDA labeled dendritic process decorated by small thorny appendages representing spines. Scale bar represents 100 µm. Scale bar on inset represents 50 µm. C-D Spatial distribution of BDA labeled cortical connections. C) One mm anterior to the injection site retrogradely labeled neurons were clustered in two groups within the supra, (upper) and infragranular (lower) cortical layers (black arrows). Scale bar represents 100 µm. D)Approximately 1 mm caudal to the injection site retrograde labeling appeared only in the supragranular layers (black arrow). Scale bar represents 100 µm.

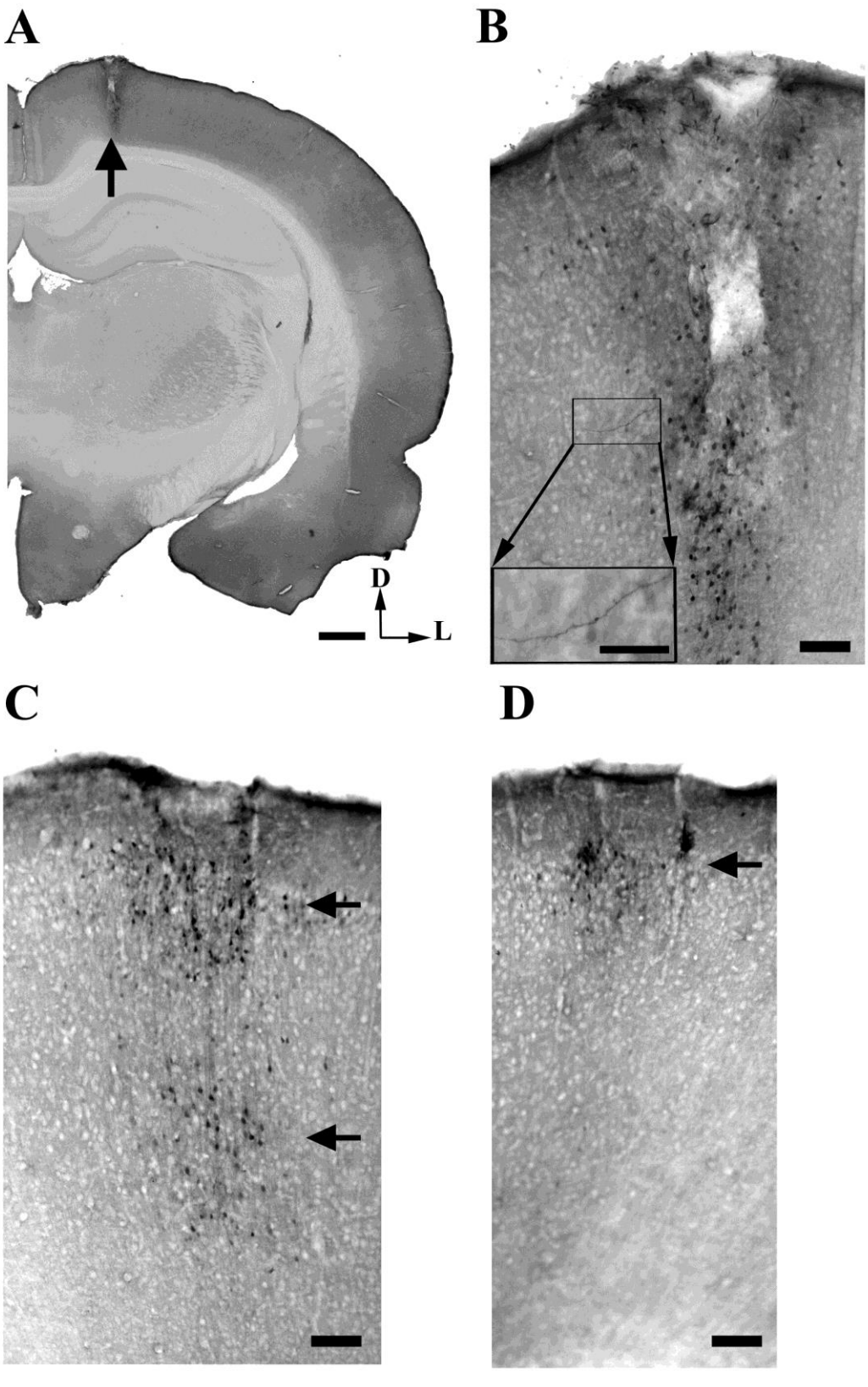

Figure 6. Samples of neuronal activity during slow wave sleep, recorded with a linear MEA after iontophoresis. The bottom signals were obtained at the location of the tracer injection. The probe was extracted from the brain tissue with 800 µm steps.

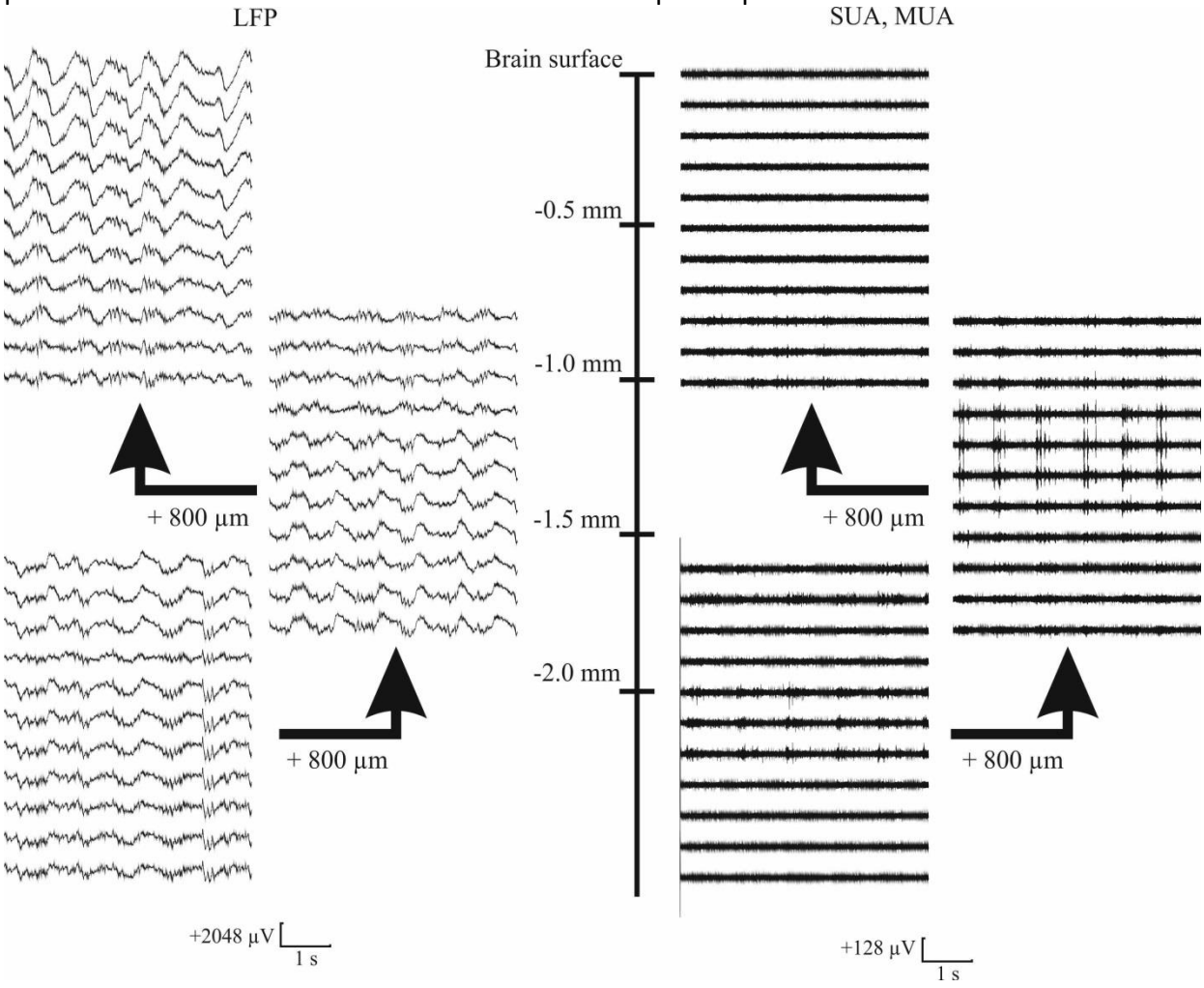

Figure 7. Detected unit activities at the location of iontophoresis (A) and 800 µm above (B). Clusters separated with two dimensional principal component analyses are shown on the left. Piled SU waveforms and average SU waveforms of unit activities in different clusters are shown on the right. Perpendicular scale bars are 20 µV.

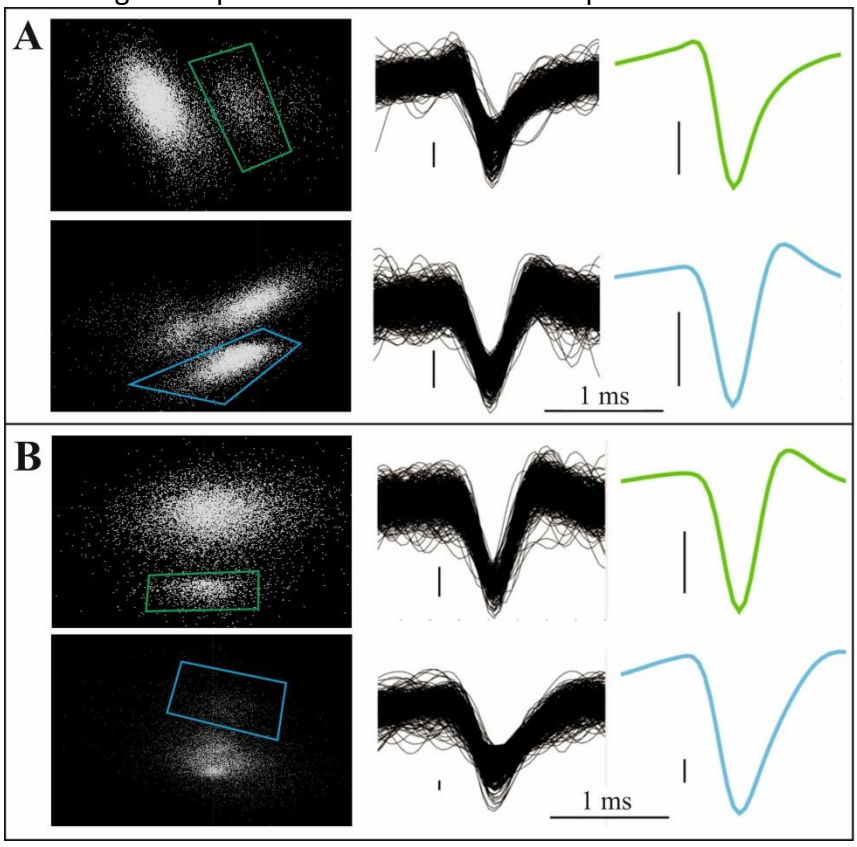

Tables

Table 1. Parameters of the applied iontophoretic injections per surgery.

Cases	Measured current (μA)	Length of ON/OFF cycles (sec)	Rat type	Weight (g)	Successful injection of BDA
REF	0	0	Wistar♂	5-600	No
LF1	1-2	12-13/5	Wistar♂	5-600	Yes
MF1	2-4	7/7	Wistar♂	510	Yes
MF2	2-4	7/7	Wistar♂	503	Yes
HF1	7-19	1/1	Wistar♂	600	Yes
HF2	1-2	1/1	Wistar♂	520	Yes

Table 2. Parameters of the iontophoretic injections for coronal sectioning to map the projectome of the primary somatosensory trunk area. The targeted depth was 1000 µm. The distance of the fluidic outlet and the counter electrode is 221 µm. The size of the counter Pt electrode is 900 μm^2. High molecular weight BDA (10.000 K) was used as a tracer. The total delivery time was 15 min. * refers to the depth until the signal of injected BDA is detected during histology.

Cases	**Measured current (µA)**	**Length of ON/OFF cycles (sec)**	**Rat type**	**Weight (g)**	**Anesthetic**	**Depth of fluidc outlet (µm)**	**Depth of BDA signal (µm)***
REF2	-	-	Wistar, female	260	0.5 ml KX (initial) 0.3 ml KX (updates)	690	-
PR	4	5/5	Wistar, female	260	0.5 ml KX (initial) 0.3 ml KX (updates)	935	1140
PRELFIZ	7	5/5	Wistar, female	260	0.5 ml KX (initial) 0.6 ml KX (updates)	850	1150

Table 3. Parameters of iontophoretic injections. The tip of the electrodes were lowered 1000 µm below the pial surface. * refers to the depth until the signal of injected BDA is detected during histology.

Cases	**Depth of the electrode track (µm)**	**Depth of the BDA injection (µm)***	**Width of the halo zone (µm)**
REF	480	660	-
LF1	1320	1440	120
MF1	1000	900	135
MF2	840	960	170
HF1	540	900	70
HF2	600	900	70